Noble-gas-related defects in Si and the origin of the 1018 meV photoluminescence line

S. K. Estreicher[*] and J. Weber

Max-Planck Institut für Festkörperforschung, 70569 Stuttgart, Germany

A. Derecskei-Kovacs and D. S. Marynick

Department of Chemistry and Biochemistry, University of Texas at Arlington, Arlington, Texas 76019

(Received 29 July 1996)

The implantation of noble-gas ions in Si results in the appearance of photoluminescence centers that are closely associated with the intrinsic-defect luminescence at 1018 meV. We present the results of a theoretical study aimed at identifying these defects. The calculations are performed in molecular clusters at the *ab initio* and approximate *ab initio* Hartree-Fock levels. Our predictions are as follows. (i) Interstitial noble-gas impurities are not associated with the luminescence and their activation energies for diffusion are large. (ii) Noble-gas atoms do not become substitutional, but are strongly repelled by vacancies instead. This suggests an unusual vacancy-enhanced diffusion mechanism. (iii) Noble-gas-divacancy complexes are very stable and their calculated properties show them to be excellent candidates as the defects responsible for the noble-gas-related photoluminescence. (iv) Larger vacancy aggregates (up to the hexavacancy) cannot be responsible for the observed luminescence, although the formation of a hexavacancy-noble-gas complex could nicely explain the disappearance of the luminescence at higher temperatures. (v) Our results imply that the 1018-meV line is due to the neutral divacancy. [S0163-1829(97)00307-X]

I. INTRODUCTION

Noble-gas (NG) elements have filled sp shells and are chemically almost inert. Comprehensive reviews of their history, properties, and chemistry can be found in Ref. 1. Some of the key properties relevant to the present study are given in Table I. The high promotion energies from the ground state to states with unpaired electrons and the high ionization enthalpies result in little or no chemical activity, especially for the lighter elements. There are no stable compounds involving He, Ne, or Ar, although the cations He_2^+ and HeH^+ have been detected by mass spectrometry.[1] Krypton forms a few compounds with F, such as KrF_2.

Xenon reacts with elements or radicals that have a large electron affinity. Xenon oxides, fluorides, oxofluorides, and a few other species are known. The oxidation numbers follow the usual "group number-2n" rule: 8 in XeO_4, 6 in XeF_6 and XeO_3, 4 in XeF_4, and 2 in XeF_2. Other compounds exist as well, such as $OXeF_4$, $RbXeF_8$, or $XeCl_2$. In all cases, the bonds involve almost exclusively sp hybrids (σ type), with little or no d- or f-electron participation. No Xe silicides have been reported.

Because of their lack of chemical activity, light NG elements are commonly employed in the processing of semiconductors. They provide inert atmospheres for the growth of the crystals or thermal anneals, and low-energy NG ions are used in dry etching, ion-beam milling,[2] sputtering, or forming thin amorphous films on crystalline surfaces. Implantation followed by thermal annealing is carried out to create "bubbles" (blistering[3]), which are efficient gettering centers.[4] The consequences of NG-ion implantation include the formation of dislocation loops and microtwins,[3,5] as well as the appearance of NG-related photoluminescence (PL) centers.[6]

Van Wieringen and Warmoltz[7] measured the diffusion coefficient of He in Si in the range 967 °C–1207 °C. They obtained $D_{He} = 0.11 \exp\{-1.27 \text{ eV}/kT\}$ cm^2/s and reported not being able to diffuse Ne through their samples.

Kaplan *et al.*[8] performed a theoretical investigation of a NG element in Si. They used extended Hückel theory (EHT)

TABLE I. Selected properties of NG elements. The atomic radius is extracted from the properties of the solid and the covalent radius is obtained by extrapolating Pauling's values or from the electronegativity equalization principle (Ref. 1). Both radii are in angstroms. The (room-temperature) ionization enthalpy and the promotion energy from the ground to the lowest open-shell state are in eV.

Property	He	Ne	Ar	Kr	Xe
atomic weight (a.u.)	4.003	20.17	39.94	83.80	131.30
atomic number	2	10	18	36	54
outer shell configuration	$1s^2$	$2s^2 2p^6$	$3s^2 3p^6$	$4s^2 4p^6$	$5s^2 5p^6$
atomic radius		1.6	1.92	1.98	2.18
covalent radius	0.4–0.6	0.70	0.94	1.10	1.30
first ionization enthalpy	24.6	21.6	15.8	14.0	12.1
$ns^2 np^6 \rightarrow ns^2 np^5 (n+1)s^1$		16.6	11.5	9.9	8.3

        <u>55</u>   5037

to calculate a potential-energy surface of interstitial He in an unsaturated cluster of 30 Si atoms. The authors found that the tetrahedral interstitial (T) site is stable and that the saddle point for interstitial diffusion is the hexagonal interstitial (H) site. The energy difference between the two sites was 1.80 eV with lattice relaxation (2.30 eV without), leading to the calculated diffusivity $D_{He} = 1.20 \times 10^{-3} \exp\{-1.80 \text{ eV}/kT\} \text{ cm}^2/\text{s}$. No level in the gap associated with interstitial He was found.

In the early 1980s, it was noticed[9,10] that NG-related defects in c-Si give rise to sharp deep-level (zero-phonon) PL peaks. These peaks shift with the NG and are closely related to the common but so far unidentified 1018-meV line, also called the I_1 or W line (see below).

Two theoretical studies of NG impurities in Si have been published shortly following the PL work. They were also EHT calculations in unsaturated Si clusters containing 42 host atoms. Interstitial NG impurities were again found[11] to be stable at the T site with a saddle point at the H site, with no energy levels in the gap. NG impurities in vacancies and divacancies[12] were also considered, but with no geometry optimization. In a divacancy, He, Ne, and Ar were assumed to remain on center, while Kr and Xe were moved along the $\langle 111 \rangle$ direction by 0.36 and 0.58 Å, respectively.

While pioneering, these calculations are heavily approximated. In situations for which it is well parametrized, EHT gives results that are at best qualitative. In the case of NGs, there are simply not enough experimental data to use in a parametrization and check its validity. Then, EHT uses a product wave function and the method cannot be made self-consistent. Further, the presence of unsaturated Si dangling bonds on the surface of the cluster results in additional uncertainties. The calculated properties of impurities and defects in Si are strongly dependent on the size of the cluster *unless* its surface is properly saturated.[13] Finally, lattice relaxations and distortions play a major, if not dominant, role. It is crucial to optimize the geometry of the crystal in the vicinity of the defect or impurity. Examples are discussed in Ref. 14.

Our calculations involve He, Ne, Ar, Kr, and Xe (the latter only as an interstitial) in the (relaxed) defect-free crystal, near (just outside) and inside a monovacancy, as well as near (just outside) and inside a divacancy. Self-interstitials are not considered in the present work because they are likely to repel NG atoms rather than covalently bind to them. Our goal is to determine if there exists a simple defect with features consistent with the observed properties of the NG-related PL centers.

Most of our calculations require the use of rather large clusters. Extensive geometry optimizations with no symmetry assumptions and many degrees of freedom must be performed. Therefore, while we intend to be as quantitative as possible, our main emphasis here is to obtain the general features of the various defect centers. For our purpose, we used the (modified) approximate *ab initio* Hartree-Fock (HF) method of partial retention of diatomic differential overlap[15] (PRDDOM).

The PRDDOM results are comparable to *minimal basis-set ab initio* HF ones, but the calculations are much faster. This allowed us to perform a large number of geometry optimizations that would have required prohibitive amount of

CPU time (if feasible at all) at the *ab initio* level. The method provides geometries, energetics, and many details of the electronic structures. However, it suffers from the drawbacks associated with all minimal basis-set techniques. In particular, the energy differences are larger than the *ab initio* ones and the electronic structures are approximate. In the case of interstitial NG impurities, for which small clusters can be used, we performed *ab initio* HF calculations with large basis sets. The comparisons show that the PRDDOM and *ab initio* results have identical qualitative features.

This paper is organized as follows. Section II contains a summary of the experimental data and Sec. III describes the methodology. Sections IV, V, and VI present the calculated properties of interstitial NG impurities, NG-vacancy pairs, and NG-divacancy complexes, respectively. Section VII discusses the larger multivacancy complexes. The summary and conclusions are in Sec. VIII.

II. SUMMARY OF THE EXPERIMENTAL INFORMATION

NG ions are implanted with typical energies of the order of several keV's. A 300 °C annealing following the implantation results[2,6] in the formation of a family of deep-level defects that give rise to PL spectra. The rich PL spectra consist of a zero-phonon line and its phonon replicas. The zero-phonon lines are closely related to the 1018-meV line and grow at its expense. They are at 1012 (He), 1014 (Ne), 1009 (Ar), 1004 (Kr), and 1001 (Xe) meV.

The 1018-meV line appears after an annealing (~ 250 °C-300 °C) of Si samples exposed to neutron irradiation, ion implantation, thermal laser anneals, or a number of other damage-inducing treatments. It is independent of the impurity content of the crystal or of the species being implanted and therefore must be caused by an intrinsic defect. The line has C_{3v} symmetry[16] and has been tentatively associated with the electron paramagnetic resonance $A3$ center[17] (believed to be a trigonal tetravacancy) as well as with the trigonal di-intersticialcy.[18]

The NG-related PL lines have the following features.[6,9,10]

(i) Piezospectroscopic studies show that they correspond to defects with trigonal (C_{3v}) symmetry in all cases except for Xe, which is associated with a tetragonal (C_{2v}) defect.

(ii) The thermal stability of the complex is relatively low: typically 450°C, but only 300°C for He. After this annealing, the PL bands disappear and a new, broad, PL band appears. The latter is independent of the NG.

(iii) The occurrence of TA phonon modes in the spectrum shows a coupling of these modes to the NG lines. This led to the suggestion[9] that NG-Si covalent bonds are formed. However, an empirical model[6,19] based only on the size of NG atoms provides a simpler explanation that involves the strain resulting from the presence of a NG atom and no covalent interaction. It is indeed unlikely that He, Ne, Ar, or Kr would bind covalently with anything, but *a priori* possible that Xe could have a positive overlap with several Si dangling bonds, although we found no Xe silicide in the literature.

(iv) Sharp zero-phonon transitions and low-energy satellites due to quasi-local modes are observed. The rich vibrational spectrum suggests a complex defect. Some modes shift with the NG isotope, while others do not. In particular, the shift of the main PL line relative to the 1018-meV line is

always toward lower energies, and the smallest shift occurs for Ne.

(v) The splitting of the NG-related PL lines under uniaxial stress is highly nonlinear and changes with the NG. Varying the stress at constant temperature shows that the intensity ratios vary much less than would be expected from the reorientation of four equivalent centers with C_{3v} symmetry. This suggests that no such reorientation occurs at temperatures below 40 K.

(vi) The energy threshold required to create the NG-related PL centers has been determined[2,20–22] and is consistent with a defect containing at most three to four vacancies.

Experimentally, it is unclear whether the defect responsible for the PL forms during the implantation and becomes PL active after the anneal or is created during the anneal.

An additional feature is worth noticing. According to standard implantation theory, the implanted NG ions should penetrate into the material to a depth of a few dozen angstroms. Instead, they are observed to penetrate[2,23] to considerable depths (~ 1 μm). The enhanced diffusion of NG atoms occurs only *during* the initial exposure, not the subsequent annealing. It is not the result of channeling because the treatment results in the formation of an amorphous layer on the surface of the crystal. Since vacancies are highly mobile[24] and are believed to be present in above-equilibrium concentrations during the etch,[25,26] vacancy-enhanced diffusion is suspected. We propose an unusual mechanism in Sec. V.

III. METHODOLOGY

The host crystal is approximated by hydrogen-saturated clusters[14] containing 14 host atoms for the *ab initio* calculations and 44 host atoms (one or two fewer with a vacancy or divacancy) for the PRDDOM ones. The 44-host-atom cluster contains 5 complete host-atom shells around a bond-centered site, and none of the first or the second nearest-neighbors (NN's) are bound to a surface saturator.

As mentioned above, the PRDDOM is fully self-consistent, contains no adjustable parameters, and provides highly reliable geometries. The population analysis provides a wealth of chemical details, such as overlaps, degrees of bonding, or Mulliken charges. However, the energetics and electronic structures are approximate. The method can handle at a uniform level of theory the elements in the first four rows of the Periodic Table. It uses a minimal basis set of Slater orbitals, to which we added a set of $3d$ orbitals for all the NN's to the vacancy or divacancy. PRDDOM is much faster than *ab initio* HF, and the use of frozen-core potentials speeds up the calculations sufficiently to allow gradient optimizations to be done routinely in large systems.

In the case of interstitial NG impurities, for which a good small cluster is available, *ab initio* HF calculations were performed in addition to the large-cluster PRDDOM ones. As shown in Sec. IV, both methods predict the same behavior with larger energy differences for PRDDOM.

The *ab initio* HF calculations were performed with Hay-Wadt (HW) core potentials[27] and a polarized split-valence (SV*) basis set for the Si atoms. The NG atoms were treated at the all-electron level, also with a SV* basis set, and the H saturators had a split-valence basis set.

TABLE II. Activation energies (eV) for diffusion of NG interstitials along a T-H-T path calculated in the small and large clusters with breathing mode lattice relaxations at both sites. The H site is able to relax more in the small cluster than in the large one (this affects the larger NG atoms). Therefore, the *ab initio* HF activation energies of Ar, Kr, and Xe are lower limits, while the (large cluster) PRDDOM ones are upper limits to the actual activation energies. The experimental number for He comes from a high-temperature permeation experiment (Ref. 7).

Method	He	Ne	Ar	Kr	Xe
PRDDOM (large)	2.11	3.06	6.50	8.47	
PRDDOM (small)	2.33	2.71	4.49	5.42	
ab initio (small)	1.38	2.03	3.51	3.88	3.93
experiment	1.27				

We tested this approach with KrF_2, XeF_2, and XeO_3, for which configurations are known[1] from experiment or near-exact theory. We optimized the geometries of the three molecules at the *ab initio* HF level and that of KrF_2 at the PRDDOM level as well. In all cases, the correct geometry and (at least qualitatively) electronic structure were obtained. In the case of KrF_2, for example, we get a linear molecule with Kr$-$F=1.86 Å (*ab initio*) and 1.94 Å (PRDDOM). In Ref. 1 the molecule is linear with Kr$-$F=1.87 Å. The *ab initio* bond order is 0.60 with overlap population $+0.05$ and the PRDDOM degree of bonding is 0.35 with overlap population $+0.05$ as well. The Mulliken charges are in both cases $+0.4$ on Kr and -0.2 on each F. These numbers are consistent with the description of the molecule in Ref. 1. Note that if the HW pseudopotentials are used for the NG atom, much longer and weaker bonds result.

IV. INTERSTITIAL NOBLE-GAS IMPURITIES

Calculations at all levels of theory predict that NG interstitials are at the T site. This is not surprising since there is no degeneracy, and the NG atoms are essentially hard balls that do not interact chemically with their environment and therefore tend to be at the roomiest interstitial site available. This result agrees with the predictions of other authors.

There is very little perturbation to the energy eigenvalues relative to the perfect cluster in the case of He and Ne, which are small and only minimally perturb the host crystal (less than 1% lattice relaxation). The presence of Ar, Kr, and Xe results in increasingly large lattice relaxations around the T site. At both levels of theory considered, the energy levels are dragged down from the conduction band and up from the valence band into the gap, which narrows as a result. The absence of deep levels and T_d symmetry imply that isolated interstitial NG are not the defect responsible for the PL.

The saddle point for the diffusion is at the H site. Again, there is very little lattice relaxation around He and Ne and larger relaxations around Ar, Kr, and Xe. The *ab initio* and PRDDOM activation energies for diffusion are given in Table II. Note that the *ab initio* value for He is close to the experimental number.

Figure 1 shows the amount of energy needed to insert a free NG atom into a T site in the cluster and allow it to relax.
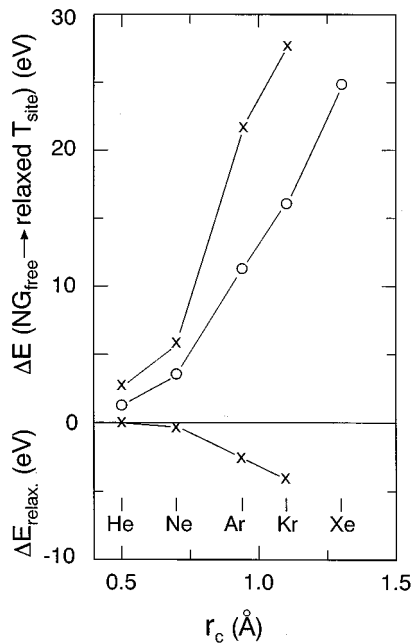
FIG. 1. Calculated cost in energy for inserting a free NG atom into the Si cluster at a (relaxed) T site. The PRDDOM energies (crosses) increase faster with the NG atom than the *ab initio* ones (circles), but the two curves are qualitatively the same. The bottom curve shows the relaxation energy at the T site calculated at the PRDDOM level. The (estimated) covalent radius (Table I) is labeled r_c.

As expected, the energies increase rapidly with the size of the NG. The high activation energies imply that only He (and maybe Ne) diffuses along T-H-T paths below the melting point of the crystal. Therefore, the isolated interstitial cannot be the rapidly diffusing species observed during the implant.

Note that PRDDOM predicts larger energy differences than large basis-set *ab initio* HF. This is mostly caused by the use of a minimal basis set and is not restricted to NG interstitials in Si. Studies[14] involving a wide range a defects and impurities in semiconductors using PRDDOM and *ab initio* HF show that the geometries and trends are nearly identical with both methods, but the energy differences obtained at the PRDDOM level are typically 30–50 % larger than the *ab initio* ones. In the case of Fig. 1, the energy for Kr is very large with the *ab initio* HF method, and the PRDDOM value is larger still. However, the trends are clearly the same.

V. NOBLE-GAS–VACANCY INTERACTIONS

The vacancy in silicon is a rapid diffuser in the -2, 0, and $+2$ charge states.[24] We consider here only the neutral charge state. The four dangling bonds reconstruct to form two stretched bonds between pairs of Si atoms, with no overlap between the atoms belonging to different pairs. Although their overlap has substantial covalent character, the reconstructed bonds are weak (see Ref. 24 for a review of the experimental work and Ref. 28 for the most recent theoretical study). The usual interaction between a vacancy and an interstitial impurity consists in the impurity becoming substitutional in order to maximize its overlap with the crystal.
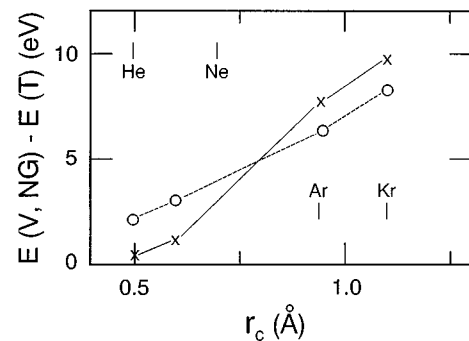

FIG. 2. The solid line shows the energy difference (eV) between the NG-vacancy pair and the isolated vacancy and interstitial NG. The dashed curve is the activation energy for diffusion of the isolated NG interstitial calculated at the same level of theory (PRDDOM, Table II). The difference between the two curves is small and roughly independent of the NG, showing that for them, the size does not matter. The (estimated) covalent radius (Table I) is labeled r_c.

Examples include the vacancy–self-interstitial annihilation and the trapping of one to four H interstitials by a vacancy.[28,29]

The case of NG's is radically different because the promotion energy from the ground to the lowest-energy open-shell configuration is very large (see Table I for the free-atom values). As a result, a NG atom in a monovacancy not only disrupts the rebonding, but is also strongly *repelled* by the electron density in the reconstructed bonds. This is a Pauli repulsion because the NG orbitals are completely full and any electron overlapping with the NG can only populate empty orbitals that are very high in energy. Attempts to optimize a configuration with a NG impurity inside a vacancy results in slow convergence and energies substantially higher than when the NG impurity remains *outside* the vacancy.

The most favorable configuration for the NG-vacancy pair has the NG outside the vacancy, off the T site. However, the electron density in the reconstructed bonds is sufficiently delocalized to render this configuration high in energy as well. The atoms try to position themselves in a way that *minimizes* any electronic overlap with the NG. Even in the best possible configuration, the NG-vacancy pair is much higher in energy than the isolated interstitial NG atom far away from a (reconstructed) vacancy. This repulsion energy is shown in Fig. 2. It increases as one goes down the Periodic Table.

Figure 2 also shows the activation energy for diffusion of the isolated interstitial NG, calculated at the same level of theory. The vacancy-NG repulsion is slightly less than this activation energy for He and Ne and slightly more for Ar and Kr. However, the difference between the two curves is not only small but also approximately independent of the NG. Thus, if a vacancy with sufficiently high kinetic energy gets close to any NG interstitial, it will repel just strongly enough to make the NG jump to a neighboring T site.

This result suggests a vacancy-enhanced diffusion mechanism that would work similarly for He, Ne, Ar, and Kr. If the flux of vacancies coming from the surface during the implantation is sufficiently energetic, the vacancies would push the NG interstitials deeper into the bulk. The activation energy for interstitial diffusion minus the repulsion energy from vacancies gives a net activation energy that is small and
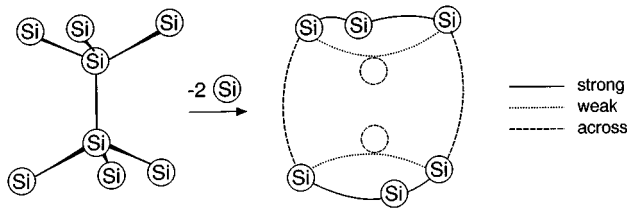
FIG. 3. Schematic diagram illustrating the reconstruction of a neutral divacancy in its lowest-energy state. Two of the six NN's form two ''strong'' bonds and each of the other four NN's forms one strong bond, one ''weak'' bond, and one ''across'' bond (see the text and Table III). There are three equivalent configurations. The dashed circles show the two missing host atoms.

roughly the same for all the NG, regardless of their size.

Note that one cannot perform Xe calculations at the PRDDO/M level. Therefore, we cannot predict its behavior near a vacancy. It is *a priori* possible that the electron affinity of the reconstructed bonds in the vacancy is high enough to ionize Xe and result in the formation of covalent bonds. However, we think that this is unlikely because Xe is too large an atom to fit in a vacancy. The net volume available is the same as at a T site and the energy needed to put a free Xe atom there is very large (see Fig. 1).

VI. NOBLE-GAS–DIVACANCY COMPLEXES

The minimum of the potential-energy surface for a neutral divacancy in Si has been calculated by gradient optimizing its six NN's with no symmetry assumption. The lowest-energy configuration is illustrated schematically in Fig. 3. The three Si atoms above and below the center of the divacancy rearrange themselves in such a way that one of the three forms a rather ''strong'' bond with its two NN's, while the other two atoms form one ''weak'' bond with each other and each makes a long bond ''across'' the divacancy. The overlap population in each of these reconstructed bonds is positive, indicating a bonding interaction.

There are three identical configurations, since the weak bond can form between any of the three possible pairs of atoms. The symmetry of the divacancy is therefore trigonal if the barrier for the rearrangement between the three equivalent configurations is small (a few hundredths of an eV are quoted for such a reorientation in Ref. 30). This rearrangement, which occurs around a fixed $\langle 111 \rangle$ axis, is accomplished by moving the six atoms by very short distances. More details about the divacancy and other vacancy cluster will be published separately.[31]

We calculated the divacancy-NG interaction by starting with a NG interstitial and a (reconstructed) divacancy in its neighborhood. Successive cyclic and gradient geometry optimization show that the NG atom penetrates into the divacancy with a substantial gain in energy and no activation energy. The energy difference between a NG interstitial far from an isolated divacancy and the NG inside the divacancy (reoptimized) is shown in Fig. 4. A comparison to the PRDDOM result in Fig. 1 shows that the NG atoms are remarkably stable in a divacancy. They are still less stable than NG atoms in free space, but only by a small amount. Thus one gains a lot of energy by forming a NG-divacancy
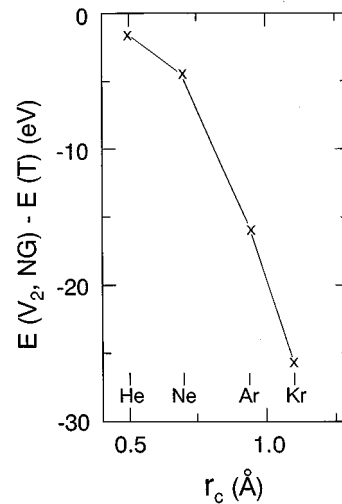

FIG. 4. Energy difference (eV) between the NG-divacancy complex and the isolated divacancy and interstitial NG. The curve was obtained with the PRDDOM. The (estimated) covalent radius (Table I) is labeled r_c.

complex and a much smaller amount of energy by going to larger vacancy aggregates.

When a NG impurity is placed in the divacancy, it remains very close to its geometrical center and only weakly perturbs its reconstruction. Table III quantifies this reconstruction. It gives the average displacement of the six NN's upon insertion of the NG relative to their position in the reconstructed divacancy, the displacement of the NG off the geometrical center of the complex, the degrees of bonding[34] and overlap population in the strong, weak, and across bonds, the average Mulliken charge on each of the six NN's, and the Mulliken charge on the NG.

The covalent character of the reconstructed bonds in the divacancy is reduced when a NG is inserted in the divacancy, but there is no change in the overall configuration. The NG impurity displaces its six NN's by a small amount, pushing them away from it. The impurity itself remains almost on center, shifting by 0.1 Å or less mostly in one of the $\{110\}$ planes common to the trigonal axis of the complex. The small value of the off-axis shift suggests that a reorientation between three equivalent configurations around the same trigonal axis can occur.

The change in the charge distribution as a function of the NG shows that the reconstructed bonds capture increasing amounts of electron density from the NG. The average Mulliken charge on each of the Si NN's varies from -0.12 to -0.16 and the charge on the NG from $+0.01$ to $+0.29$ as one goes from He to Kr. As shown in Table I, the ionization enthalpies decrease from He to Kr, making it easier for the reconstructed bonds to grab some charge from the NG. This trend should continue with Xe. If enough electron density is removed from it, Xe could well covalently overlap with some Si atoms in the divacancy resulting in a change of configuration. Large basis-set *ab initio* calculations will be needed to confirm this point.

The energy eigenvalues are more difficult to interpret because of the approximations involved in the HF methodology. In particular, the ''conduction band'' and the unoccupied ''gap'' states are arbitrarily high in energy. We know of

TABLE III. Perturbation of the (reconstructed) divacancy by a NG impurity. The table gives the post-reconstruction average displacement of the NN's to the NG, the displacement of the NG from the geometrical center of the divacancy, the degrees of bonding and overlap populations for the strong, weak, and across bonds (see Fig. 3), the average Mulliken charge on each NN, and the Mulliken charge on the NG.

	Divacancy	He	Ne	Ar	Kr
			displacement (Å)		
each NN (avg.)	0.00	0.05	0.07	0.23	0.27
NG (off center)	–	0.07	0.09	0.11	0.06
			degree of bonding/overlap population		
strong bond	0.49/0.20	0.48/0.18	0.46/0.16	0.41/0.09	0.40/0.08
weak bond	0.07/0.04	0.07/0.04	0.06/0.03	0.07/0.01	0.03/0.01
across bond	0.18/0.02	0.19/0.01	0.20/0.01	0.16/0.00	0.14/0.00
			Mulliken charge ($|e|$)		
each NN (avg.)	-0.11	-0.12	-0.13	-0.14	-0.16
NG	–	$+0.01$	$+0.08$	$+0.22$	$+0.29$

no method able to predict the position of deep levels in the gap with the accuracy needed to make quantitative predictions of a PL spectrum (in the present case, the shifts of the NG-related PL lines are of the order of the meV). In our calculations, the use of a minimal basis set adds to the uncertainties. We will therefore limit ourselves to qualitative statements about the energy eigenvalues.

The neutral divacancy and each of the NG-divacancy complexes have six levels in the gap, three of which are doubly occupied. They correspond to the bonding and antibonding levels of the six electrons in the reconstructed bonds. The positions of these levels shift with the NG. In each case, there are at most nine possible excitations involving these levels. We calculated these excitations energies and their shift with the NG relative to the ones in the perfect divacancy. All the shifts are toward lower energies. Some of them are almost independent of the NG, while others vary considerably. Some vary monotonically with the size of the impurity. However, two of the shifts have a trend identical to that of the zero-phonon line discussed by Davies *et al.*[19] in their model based on internal strain generated by the NG.

While we are well aware that one should be extremely careful not to trust such numbers too much, the overall features of the energy eigenvalues are compatible with the existence of the PL spectrum and with shifts relative to the unperturbed center that are qualitatively similar to the ones observed.

VII. LARGER VACANCY AGGREGATES

In a separate study,[31] we have calculated the formation energies and stable configurations of vacancy aggregates up to the heptavacancy. Note that experiment[2,20,21] indicates that the NG-related defects contain at most three to four vacancies. Our calculations therefore cover all the possible vacancy clusters.

Molecular-dynamics simulations[31] show that in their lowest-energy configurations, only the divacancy and the hexavacancy can have trigonal symmetry. The trigonal symmetry of the PL lines rules out the tri-, tetra-, penta-, and heptavacancies. In its lowest-energy configuration, the reconstructed hexavacancy is the most stable of all the small

vacancy clusters, confirming empirical estimates.[32,33] We performed calculations[31] with PRDDOM, large-basis-set *ab initio* HF, and local-density-functional-based molecular-dynamics simulations for the hexavacancy. The results are that the lowest-energy configuration of the hexavacancy occurs when the missing atoms come off of one hexagonal ring in the crystal. This defect is able to reconstruct very efficiently. A comparison of energy eigenvalues obtained at all three levels of theory shows obtained that the hexavacancy has no deep levels in the gap, in contrast to the other vacancy clusters (mono- to heptavacancy). Therefore the hexavacancy should not give rise to sharp PL lines. However, band tailing (from the conduction band into the upper part of the gap) suggests that a broad PL spectrum could be associated with it. Thus only the divacancy and the NG-divacancy complexes are compatible with the sharp, trigonal PL data.

The stability of the hexavacancy and the large empty volume available in it could, however, explain the irreversible disappearance of the NG-related PL lines after 450 °C annealings. The large gain in energy resulting from the formation of the NG-divacancy complex makes it highly unlikely that it dissociates. Instead, vacancies and/or divacancies could cluster around the NG-divacancy complex and form stable NG-hexavacancy centers.

VIII. SUMMARY AND DISCUSSION

We have performed approximate *ab initio* HF calculations in large molecular clusters for He, Ne, Ar, and Kr in crystalline Si. In the case of the isolated interstitial, we have also performed *ab initio* HF calculations and included Xe, but in a smaller cluster. The other defects we studied are the NG-vacancy pair and the NG-divacancy complex. We also discussed larger vacancy-NG aggregates.

The lowest-energy site for interstitial NG impurities is at the relaxed *T* site. The activation energy for *T-H-T* diffusion increases rapidly with the size of the NG. Only interstitial He should diffuse any measurable distance at high temperatures. There is no electrical activity associated with interstitial NG

impurities, except that the lattice relaxations around the larger ones result in a narrowing of the gap.

NG impurities are strongly repelled by monovacancies. The electron density associated with the reconstructed bonds results in a Pauli repulsion between them and the filled shells of the NG. The most stable configuration of a NG and a vacancy has the NG at an interstitial site far away from the vacancy.

The energy required to bring a monovacancy to the immediate vicinity of an interstitial NG increases with the size of the NG. The magnitude of the repulsion energy is very similar to the activation energy for diffusion of the isolated interstitial. This coincidence suggests an unusual mechanism of enhanced diffusion of the NG impurities. If the implantation itself causes an above-equilibrium flux of vacancies to flow from the surface into the bulk, the vacancy-NG repulsion is large enough to overcome the barrier for diffusion. The NG interstitials would simply be pushed into the bulk by the wave of vacancies coming from the surface.

All NG impurities are remarkably stable in a neutral divacancy. The large drop in energy resulting from the formation of a NG-divacancy complex suggests that the post-implantation annealing is needed to increase the diffusivity of divacancies, which then seek out and trap NG interstitials. The trapping itself involves no activation energy. This implies that the PL-related defects do not form during the implant, but instead during the annealing that follows the implant. Note that the migration energy of the divacancy[30] (~ 1.3 eV) is consistent with the 300 °C annealing needed for the PL centers to appear.

The NG impurities perturb only slightly the reconstructed divacancy. No change in the electronic configuration results, but the reconstructed bonds are weakened. This result validates the strain-based model proposed by Davies *et al.*[6,19] to explain the shifts of the main PL peak relative to the 1018-meV line as one goes from He to Kr.

The absolute minimum of the potential-energy surface for the neutral divacancy and NG-divacancy complexes has low symmetry. This allows an optimum reconstruction to take place. However, there are in each case three equivalent configurations around the same $\langle 111 \rangle$ axis, which average out to trigonal symmetry. They differ by very small displacements ($\leqslant 0.1$ Å) of a few atoms, allowing an exchange of the strong, weak, and across bonds to occur (see Fig. 3). Molecular-dynamics simulations will be needed to actually prove that the complex easily hops between the three low-symmetry configurations and averages out to trigonal symmetry. However, the complex is much too large to reorient easily from one trigonal axis to another.

The charge exchange between the NG and the reconstructed bonds increases as one goes down the Periodic Table. In particular, Kr in the divacancy has a Mulliken charge of about $+0.3$, just short of its charge in KrF_2 ($+0.4$), where it forms a covalent bond. The trends strongly suggest that Xe in a divacancy would become even more ionized, maybe enough to form covalent bonds with some or all of its six Si NN's. This would result in a change in the electronic configuration and possibly a different symmetry for the complex.

The presence of deep levels in the gap is consistent with the existence of sharp zero-phonon lines. Further, the shifts relative to the divacancy of the differences between the calculated gap levels show trends that are qualitatively identical to the ones reported experimentally.

Up to the heptavacancy, there are no other NG-vacancy complexes that combine the existence of levels deep in the gap and trigonal symmetry. We therefore conclude that the 1018-meV defect-related line is due to the divacancy and that the NG-related lines are NG-divacancy complexes.

Our calculations imply that the NG-related PL centers do not form during the implant but during the subsequent anneal. Further, their disappearance above 450 °C cannot be caused by a breakup of the complex. As can be seen in Fig. 4, the stability of the complex relative to a divacancy and an isolated interstitial NG is much too high. However, the complex may capture more (di)vacancies up to the very stable hexavacancy.

We did not include self-interstitials in our calculations and therefore cannot rule out that they play a role. However, there is a strong repulsion between NG atoms and an electron density such as the one associated with Si dangling orbitals.

Our results suggest further experiments on the NG luminescence to verify the proposed divacancy model.

(i) The rich phonon spectrum of the NG luminescence is associated with lattice modes and local modes. In particular, one mode at around 70 meV below the 1018-meV line exhibits an isotope splitting caused by the vibration of a Si atom in the complex.[19] It is not known if the NG defects show the same Si isotope splitting (there is only one report[9] of a Ne isotope splitting of one phonon line). In its ground state, the neutral divacancy has no symmetrically unique Si atom. More details about this would be useful.

(ii) The uniaxial stress measurements on the NG-related PL centers find very small stress couplings.[35] A theoretical evaluation of the force constants of the divacancy with and without a NG impurity could explain why.

(iii) The divacancy can be reoriented[36] by uniaxial stress from one trigonal axis to another at 200 °C. If this reorientation occurs via the breakup of the divacancy, our calculations show that it would cost considerably more energy to achieve such a reorientation with a NG in the divacancy (maybe with the exception of He).

(iv) Experiments could be designed to study how the penetration depth of NG impurities is affected by the vacancies and how it varies from He to Kr.

(v) Hydrogenation[37] passivates the NG-related centers. This reaction is reversible by annealing around 350 °C. A theoretical study of the passivation/reactivation process(es) is lacking.

(vi) The annealing of the NG-related PL spectrum at higher temperatures leads to the appearance of broad, PL features with spectral position independent of the NG. A correlation with the hexavacancy could be attempted.

---

[*]Permanent address: Physics Department, Texas Tech University, Lubbock, TX 79409.

[1]*Comprehensive Inorganic Chemistry*, edited by J.C. Bailar, H.J. Emeléus, Sir R. Nyholm, and A.F. Trotman-Dickenson (Pergamon, Oxford, 1973), Vol. 1; F.A. Cotton and G. Wilkinson, *Inorganic Chemistry*, 5th ed. (Wiley, New York, 1988), and references therein.

[2]For a recent review, see J. Weber, Physica B **170**, 201 (1991).

[3]K. Wittmaack and W. Wuch, Appl. Phys. Lett. **32**, 532 (1978).

[4]S.M. Myers, D.M. Follstaedt, H.J. Stein, and W.R. Wampler, Phys. Rev. B **45**, 3914 (1992); H.J. Stein, S.M. Myers, and D.M. Follstaedt, J. Appl. Phys. **73**, 2755 (1993).

[5]P. Revesz, M. Wittmer, J. Roth, and J.W. Mayer, J. Appl. Phys. **49**, 5199 (1978).

[6]G. Davies, Phys. Rep. **176**, 83 (1989).

[7]A. Van Wieringen and N. Warmoltz, Physica **22**, 849 (1956).

[8]D.R. Kaplan, C. Weigel, and J.W. Corbett, Phys. Status Solidi B **94**, 359 (1979).

[9]V.D. Tkachev, A.V. Mudryi, and N.S. Minaev, Phys. Status Solidi A **81**, 313 (1984), and references therein.

[10]N. Bürger, K. Thonke, R. Sauer, and G. Pensl, Phys. Rev. Lett. **52**, 1645 (1984).

[11]A.V. Mudryi, A.L. Pushkarchuk, V.D. Tkachev, and A.G. Ul'yashin, Phys. Status Solidi B **125**, K75 (1984); Fiz. Tekh. Poluprovodn. **18**, 1676 (1984) [Sov. Phys. Semicond. **18**, 1048 (1984)].

[12]A.V. Mudryi, A.L. Pushkarchuk, and A.G. Ul'yashin, Fiz. Tekh. Poluprovodn. **19**, 360 (1985) [Sov. Phys. Semicond. **19**, 225 (1985)].

[13]See, e.g., S.K. Estreicher, A.K. Ray, J.L. Fry, and D.S. Marynick, Phys. Rev. Lett. **55**, 1976 (1985).

[14]S.K. Estreicher, Mat. Sci. Engr. Rep. **14**, 319 (1995).

[15]For the latest developments in the PRDDO methodology, see A. Derecskei-Kovacs and D.S. Marynick, Int. J. Quantum. Chem. **58**, 193 (1996); A. Derecskei-Kovacs, D.E. Woon, and D.S. Marynick, Int. J. Quantum. Chem. (to be published).

[16]N.S. Minaev, A.V. Mudryi, and V.D. Tkachev, Phys. Status Solidi B **108**, K89 (1981).

[17]Y.H. Lee and J.W. Corbett, Phys. Rev. B **9**, 4351 (1974).

[18]J.W. Corbett, J.C. Bourgoin, and C. Weigel, IOP Conf. Ser. **16**, 1 (1973).

[19]G. Davies, E.C. Lightowlers, and Z.E. Ciechanowska, J. Phys. C **20**, 191 (1987).

[20]W.D. Sawyer, J. Weber, G. Nabert, J. Schmälzlin, and H.-U. Habermeier, J. Appl. Phys. **68**, 6179 (1990).

[21]W.D. Sawyer and J. Weber, in *Scientific Basis for Nuclear Waste Management XIII*, edited by V.M. Oversby and P.W. Brown, MRS Symposia Proceedings No. 176 (Materials Research Society, Pittsburgh, 1990), p. 197.

[22]W.D. Sawyer (private communication).

[23]J. Weber and W.D. Sawyer, in *Defect Control in Semiconductors*, edited by K. Sumino (Elsevier, Amsterdam, 1990), p. 513.

[24]G.D. Watkins, in *Deep Centers in Semiconductors*, edited by S.T. Pantelides (Gordon and Breach, New York, 1986), p. 147.

[25]J.W. Corbett, J.L. Lindström, and S.J. Pearton, in *Defects in Electronic Materials*, edited by M. Stavola, S.J. Pearton, and G. Davies, MRS Symposia Proceedings No. 104 (Materials Research Society, Pittsburgh, 1988), p. 229.

[26]B.L. Sopori, X. Deng, J.P. Benner, A. Rohatgi, P. Sana, S.K. Estreicher, Y.K. Park, and M.A. Roberson, Solar En. Mater. Solar Cells **41/42**, 159 (1996).

[27]P.J. Hay and W.R. Wadt, J. Chem. Phys. **82**, 270 (1985).

[28]M.A. Roberson and S.K. Estreicher, Phys. Rev. B **49**, 17 040 (1994); Y.K. Park, S.K. Estreicher, C.W. Myles, and P.A. Fedders, *ibid.* **52**, 1718 (1995).

[29]B. Bech Nielsen, L. Hoffmann, M. Budde, R. Jones, J. Goss, and S. Öberg, Mater. Sci. Forum **196-201**, 933 (1995).

[30]J.W. Corbett in *Electron Radiation Damage in Semiconductors and Metals* (Academic, New York, 1966).

[31]S.K. Estreicher, J.H. Hastings, and P.A. Fedders, Appl. Phys. Lett. **70** (to be published); and J.L. Hastings, S.K. Estreicher, and P.A. Fedders (unpublished).

[32]D.J. Chadi and K.J. Chang, Phys. Rev. B **38**, 1523 (1988).

[33]A. Oshiyama, M. Saito, and O. Sugino, Appl. Surf. Sci. **85**, 239 (1995).

[34]D.R. Armstrong, P.G. Perkins, and J.J.P. Stewart, J. Chem. Soc. Dalton Trans. 838 (1973).

[35]N. Bürger, E. Irion, A. Teschner, K. Thonke, and R. Sauer, Phys. Rev. B **35**, 3804 (1987).

[36]V.D. Tkachev and A.V. Mudryi, in *Radiation Damage Defects in Semiconductors*, edited by N.B. Urli and J.W. Corbett, IOP Conf. Proc. No. 31 (Institute of Physics and Physical Society, London, 1977), p. 231.

[37]J. Weber (unpublished).